

We are IntechOpen, the world's leading publisher of Open Access books Built by scientists, for scientists

6,900

Open access books available

186,000

International authors and editors

200M

Downloads

Our authors are among the

154

Countries delivered to

TOP 1%

most cited scientists

12.2%

Contributors from top 500 universities



WEB OF SCIENCE™

Selection of our books indexed in the Book Citation Index
in Web of Science™ Core Collection (BKCI)

Interested in publishing with us?
Contact book.department@intechopen.com

Numbers displayed above are based on latest data collected.
For more information visit www.intechopen.com



Thermodynamic Properties of the Polyols as Phase Change Materials for Thermal Energy Storage

Zhicheng Tan, Quan Shi and Xin Liu

Additional information is available at the end of the chapter

<http://dx.doi.org/10.5772/intechopen.78800>

Abstract

In this chapter, four natural polyhydroxy alcohols (polyols), including xylitol, sorbitol, adonitol, and erythritol were selected as the subject of study on phase change materials for thermal energy storage application. The thermodynamic study on these polyols was performed by adiabatic calorimetry (AC), differential scanning calorimetry (DSC), and thermogravimetric analysis (TG). The heat capacities of these polyols were measured in the temperature range from 80 to 400 K by a fully automated high-precision adiabatic calorimeter. The experimental heat capacities of these polyols were fitted to the polynomial equations of heat capacities as a function of temperatures. The thermodynamic property data, such as temperatures, enthalpies, and entropies of the phase transitions, were obtained based on the experimental heat capacities in the phase transition temperature range. According to the thermodynamic relation equations, the standard thermodynamic functions of these polyols, relative to the standard reference temperature 298.15 K, $[H_T - H_{298.15}]$ and $[S_T - S_{298.15}]$, were calculated with the interval of 5 K. The thermal stability and heat storage capacity of the polyols were also investigated by thermal analysis.

Keywords: phase change material (PCM), polyhydroxy alcohol (polyol), natural polyol, thermodynamic properties, heat capacity, temperature of phase transition, enthalpy and entropy of phase transition, adiabatic calorimetry (AC), thermal analysis, DSC, TG

1. Introduction

In recent two decades, the phase change materials (PCMs) have attracted much attention due to their remarkable effects to thermal energy storage applications. It has been demonstrated that the research of PCMs is becoming one of the most hot research topic in the world. The basic theory of PCMs application is utilizing the heat energy being absorbed or released when

the phase transition processes take place at a constant temperature. Consequently, the thermodynamic properties of PCMs, especially the heat capacity, phase transition temperature, and enthalpy would play a crucial role in both theoretically and technically investigating the thermal energy storage unit and its performance by using PCMs [1].

Thermal energy storage technology has wide application prospects in solar energy utilization, power generation, waste heat recovery, and utilization. Phase change material is the prerequisite for the development of thermal energy storage system, so the study of phase change materials for latent thermal energy storage application is the core subject in this field.

The polyhydroxy alcohols (polyols) have multiple hydroxyl structures, so hydrogen bonds can be formed between the molecules, and then the enthalpy of phase transition is larger. Polyols as heat storage material have many advantages, such as high phase change enthalpy, wide phase change temperature range, high mass heat storage capacity, lower super cooling degree, long service life, nontoxic, noncorrosive, etc. [2]. Therefore, as a new kind of PCMs for energy storage, polyols have been paid more and more attention. The research on basic theory and practical application of polyols has been widely carried out in the world [3–25].

The thermodynamic properties are significant for practical application of PCMs in thermal energy storage. Hence, the thermodynamic studies of PCMs have been performed in our thermochemistry laboratory for nearly 20 years long [1]. In the last decade, we have carried out the thermodynamic study of polyol as phase change materials [2]. A series of polyols, which are easily obtained and have great technical and economic potential for application, were selected as PCMs for energy storage application. The thermodynamic properties of these polyols were studied in detail using high-precision automatic adiabatic calorimeter (AC), differential scanning calorimeter (DSC), and thermogravimetric analyzer (TG), respectively [2, 16–23].

In this chapter, we report our research results on thermodynamic properties of four natural polyols: xylitol, sorbitol, adonitol, and erythritol, and introduce the modern advanced experimental calorimetric techniques used for thermodynamic studies of phase change materials.

2. Experimental

2.1. Adiabatic calorimetry and heat capacity measurements

Adiabatic calorimetry is the most accurate approach to obtain the heat capacity data. In the present study, heat capacity measurements were carried out by a high-precision automatic adiabatic calorimeter over the temperature range 80–400 K. The adiabatic calorimeter was established by Thermochemistry Laboratory of Dalian Institute of Chemical Physics, Chinese Academy of Sciences in PR China. The structure and principle of the adiabatic calorimeter have been described in detail elsewhere [26, 27]. The schematic diagram of the adiabatic calorimeter is shown in **Figure 1**. Briefly, the automatic adiabatic calorimeter is mainly composed of a sample cell, a miniature platinum resistance thermometer, an electric heater, the inner and outer adiabatic shields, two sets of six-junction chromel-constantan thermopiles installed between the calorimetric cell and the inner shield and between the inner and the

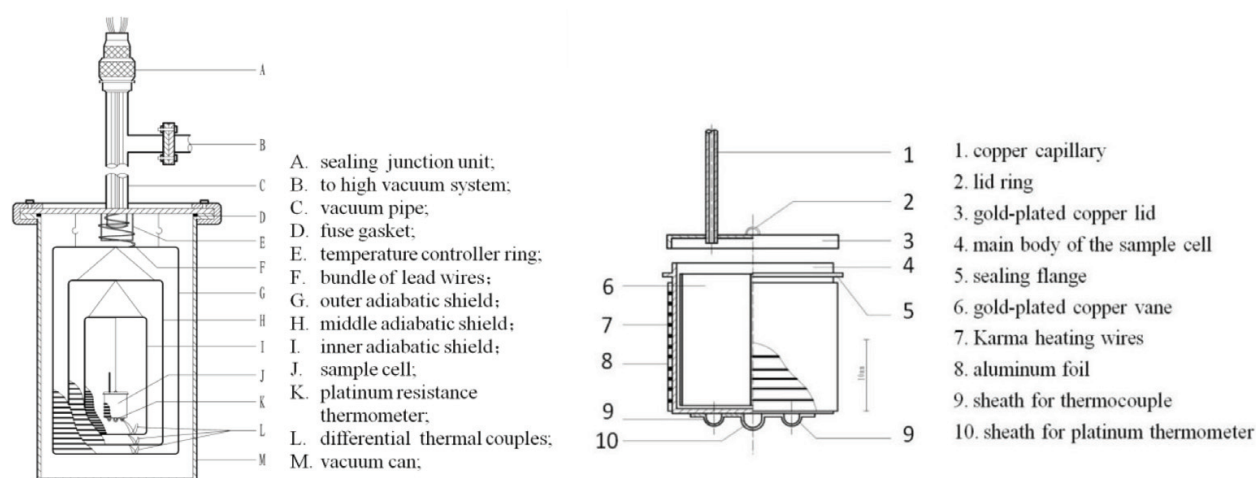


Figure 1. Schematic diagram of main body of the adiabatic calorimeter (left); schematic diagram of sample cell of the adiabatic calorimeter (right).

outer shields, respectively, and a high vacuum can. The working temperature range is 78–400 K and, if necessary, it can be cooled by liquid nitrogen. The heat capacity measurements were conducted by the standard procedure of intermittently heating the sample and alternately measuring the temperature. The heating rate and the temperature increments of the experimental points were generally controlled at $0.1\text{--}0.4\text{ K}\cdot\text{min}^{-1}$ and at 1–4 K, respectively, during the whole experimental process. The heating duration was 10 min, and the temperature drift rates of the sample cell measured in an equilibrium period were kept within $10^{-3}\text{--}10^{-4}\text{ K}\cdot\text{min}^{-1}$ during the acquisition of heat capacity data.

In order to verify the reliability of the adiabatic calorimeter, the molar heat capacities $C_{p,m}$ of the Standard Reference Material (SRM-720) ($\alpha\text{-Al}_2\text{O}_3$) were measured in the range from 78 to 400 K. The deviation of our calibration data from those of NIST [28] was within $\pm 0.1\%$ (standard uncertainty).

In the present study, the heat capacity measurements were conducted by means of the standard method of intermittently heating the sample and alternately measuring the temperature. The temperature difference between the sample and adiabatic shield was automatically kept to be about 10^{-3} K during the whole experiment. The temperature increment for a heating period was about 3 K, and temperature drift was maintained about $10^{-4}\text{ K}\cdot\text{min}^{-1}$ during each equilibrium period. The data were automatically collected through a Data Acquisition/Switch Unit (Model: 34420, Agilent USA) and processed online by a personal computer according to the program developed in our thermochemistry laboratory [26].

2.2. DSC and TG analysis

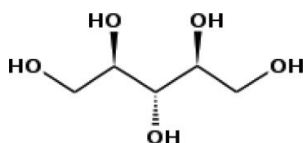
A differential scanning calorimeter (Model: DSC141, SETARAM, France) was used to perform the thermal analysis of the natural polyols under high-purity nitrogen (99.999%) with a flow rate of $40\text{ ml}\cdot\text{min}^{-1}$ and heating rate of $10\text{ K}\cdot\text{min}^{-1}$. The DSC141 was calibrated with indium and zinc standards.

The thermogravimetric measurements of the natural polyols were carried out by a TG analyzer (Model: Setaram setsys 16/18, SETARAM, France) under high-purity nitrogen (99.999%) with a flow rate of $40 \text{ ml} \cdot \text{min}^{-1}$ and heating rate of $10 \text{ K} \cdot \text{min}^{-1}$. The TG analyzer was calibrated by calcium oxalate standards.

3. Thermodynamic properties of nature xylitol: $\text{C}_5\text{H}_{12}\text{O}_5$ [(CH₂ OH) (CHOH)₃ (CH₂OH), CAS No. 87-99-0]

3.1. Sample

The xylitol sample was purchased from ACROS ORGANICS company with labeled purity >99% mass fraction. The sample was recrystallized and then purified by sublimation. It was handled in a dry N₂ atmosphere to avoid possible contamination by moisture. The chemical structure of xylitol is as follows:



The mass of the xylitol sample, used for heat capacity measurement was 4.87213 g, which is equivalent to 32.022 m mol based on its molar mass of $152.1457 \text{ g} \cdot \text{mol}^{-1}$.

The mass of the xylitol sample used in the DSC experiment was 3.48 mg, and in the TG analysis was 8.35 mg, respectively.

3.2. Results and discussion

3.2.1. Heat capacity

Experimental molar heat capacities of xylitol measured by the adiabatic calorimeter over the temperature range from 80 to 390 K are plotted in **Figure 2**. From **Figure 2**, a phase transition was observed in the range of 360–375 K with the peak heat capacity at 369.04 K. According to its melting point 365.7 K [7], this transition corresponds to a solid-liquid phase change.

The values of experimental heat capacities can be fitted to the following polynomial equations with least square method:

For the solid phase over the temperature range 80–360 K:

$$\begin{aligned} C_{p,m}^0 / \text{J} \cdot \text{K}^{-1} \cdot \text{mol}^{-1} = & 165.87 + 105.19x + 1.8011x^2 - 41.445x^3 - 41.851x^4 \\ & + 65.152x^5 + 66.744x^6 \end{aligned} \quad (1)$$

where X is the reduced temperature $x = [T - (T_{\max} + T_{\min})/2]/[(T_{\max} - T_{\min})/2]$, T is the experimental temperature, thus, in the solid state (80–360 K), $x = [(T/K) - 220]/140$, T_{\max} is the upper limit (360 K) and T_{\min} is the lower limit (80 K) of the above temperature region. The correlation coefficient of the fitting $R^2 = 0.9947$.

For the liquid phase over the temperature range 370–390 K:

$$C_{p,m}^0 / \text{J} \cdot \text{K}^{-1} \cdot \text{mol}^{-1} = 426.19 + 5.6366x \quad (2)$$

where x is the reduced temperature, $x = [(T/K) - 380]/10$, T is the experimental temperature, 380 is obtained from polynomial $(T_{\max} + T_{\min})/2$, 10 is obtained from polynomial $(T_{\max} - T_{\min})/2$. T_{\max} and T_{\min} are the upper (390 K) and lower (370 K) limit temperatures, respectively. The correlation coefficient of the fitting $R^2 = 0.993$.

3.2.2. The temperature, enthalpy, and entropy of solid-liquid phase transition

The standard molar enthalpy and entropy of the solid-liquid transition $\Delta_{\text{fus}}H_m^0$ and $\Delta_{\text{fus}}S_m^0$ of the compound were derived according to Eqs. (3) and (4):

$$\Delta_{\text{fus}}H_m^0 = \frac{Q - n \int_{T_i}^{T_m} C_{p,m}^0(s) dT - n \int_{T_m}^{T_f} C_{p,m}^0(l) dT - \int_{T_i}^{T_f} H^0 dT}{n} \quad (3)$$

$$\Delta_{\text{fus}}S_m^0 = \frac{\Delta_{\text{fus}}H_m^0}{T_m} \quad (4)$$

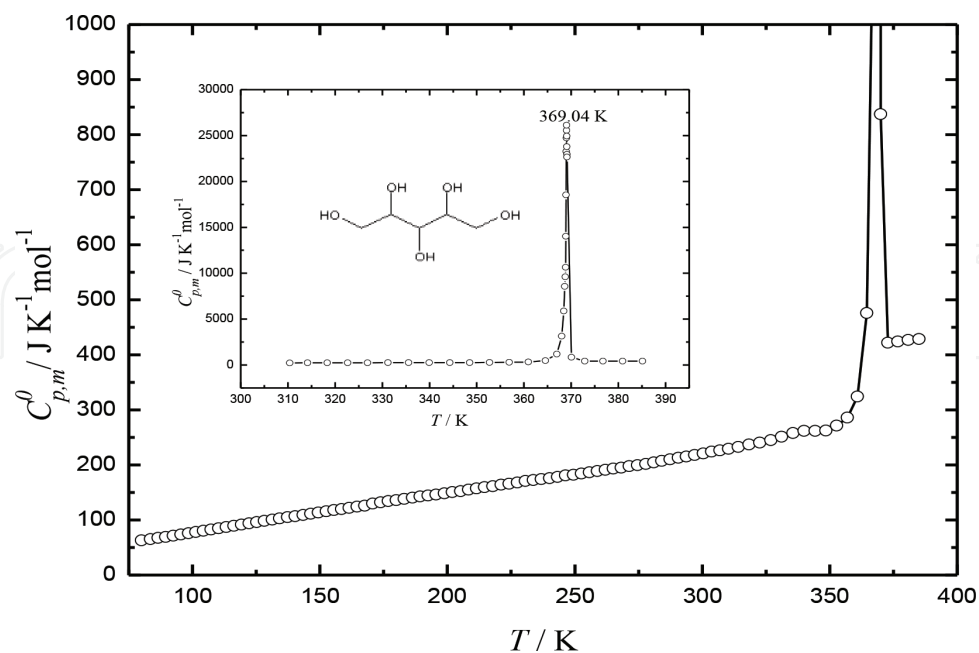


Figure 2. Experimental molar heat capacity of xylitol as a function of temperature.

where T_i is the temperature that is somewhat lower than the temperature of the onset of a solid-liquid transition and T_f is the temperature slightly higher than that of the transition completion. Q is the total energy introduced into the sample cell from T_i to T_f , H^0 , the standard heat capacity of the sample cell from T_i to T_f , $C_{p,m}^0(s)$, the standard heat capacity of the sample in solid phase from T_i to T_m , $C_{p,m}^0(l)$, the standard heat capacity of the sample in liquid phase from T_m to T_f and n is the molar amount of the sample. The heat capacity polynomials mentioned above were used to calculate the smoothed heat capacities, and were numerically integrated to obtain the values of the standard thermodynamic functions above $T = 298.15$ K. The calculated results can be found in our previous publication [17].

The thermodynamic functions of the xylitol relative to the reference temperature 298.15 K were calculated in the temperature range 80–390 K with an interval of 5 K, using the polynomial equation of heat capacity and thermodynamic relationships as follows:

Before melting,

$$H_T^0 - H_{298.15}^0 = \int_{298.15}^T C_{p,m}^0(s) dT \quad (5)$$

$$S_T^0 - S_{298.15}^0 = \int_{298.15}^T \frac{C_{p,m}^0(s)}{T} dT \quad (6)$$

After melting,

$$H_T^0 - H_{298.15}^0 = \int_{298.15}^{T_i} C_{p,m}^0(s) dT + \Delta_{fus} H_m^0 + \int_{T_f}^T C_{p,m}^0(l) dT \quad (7)$$

$$S_T^0 - S_{298.15}^0 = \int_{298.15}^T \left[\frac{C_{p,m}^0(s)}{T} \right] dT + \frac{\Delta_{fus} H_m^0}{T_m} + \int_{T_f}^T \left[\frac{C_{p,m}^0(l)}{T} \right] dT \quad (8)$$

where T_i is the temperature at which the solid-liquid phase transition started; T_f is the temperature at which the solid-liquid phase transition ended; $\Delta_{fus} H_m^0$ is the standard molar enthalpy of fusion; T_m is the temperature of solid-liquid phase transition. The standard thermodynamic functions, $H_T^0 - H_{298.15}^0$ and $S_T^0 - S_{298.15}^0$ can be consequently calculated based on the equations [17].

3.2.3. The result of TG and DSC analysis

From the DSC curve in **Figure 3**, a sharply endothermic peak corresponding to melting process was observed, with the peak temperature of 367.52 K and the enthalpy of 33.68 ± 0.34 kJ·mol⁻¹, which are consistent with the values 369.04 K, 33.26 ± 0.17 kJ·mol⁻¹ observed from the adiabatic calorimetric measurements. The results were listed in Ref. [17], from which, it can be seen that the standard thermodynamic parameters obtained from adiabatic calorimetry and DSC in the present research are in accordance with each other and slightly lower than those reported in literature [4].

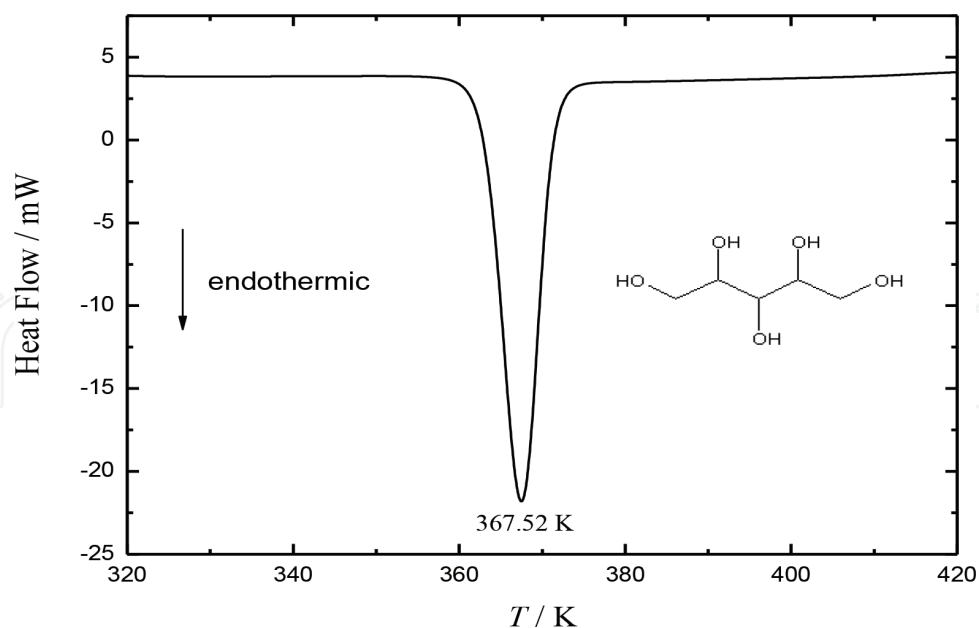


Figure 3. DSC curve of xylitol under high-purity nitrogen.

From the TG curve in **Figure 4**, it can be seen that the mass loss of the sample was completed in a single step. The sample keeps thermostable below 400 K. It begins to lose weight at 451.20 K, reaches the maximum rate of weight loss at 617.13 K, and completely loses its weight when the temperature reaches 675.30 K.

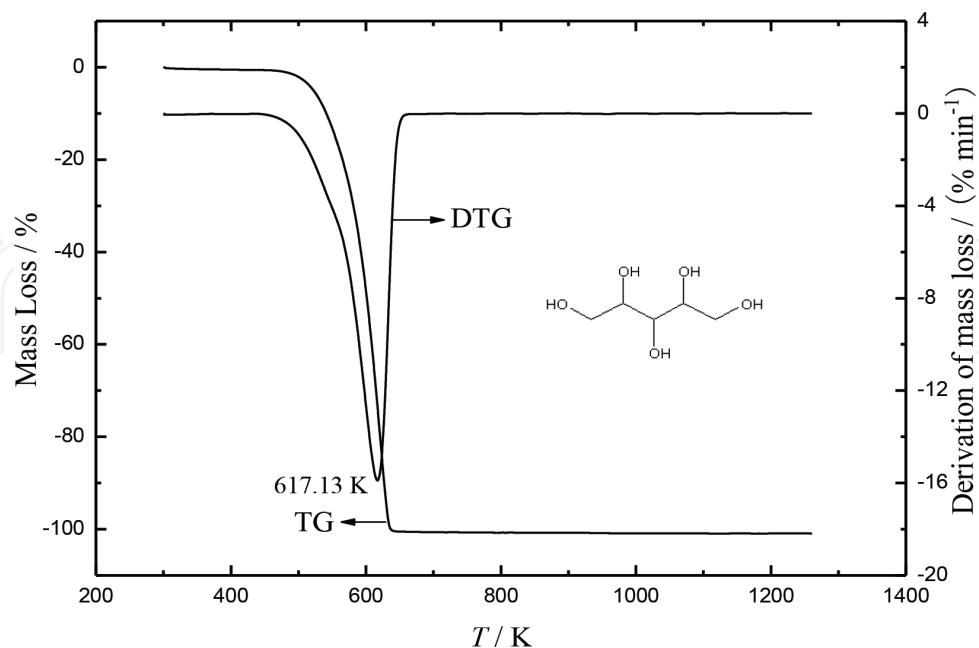


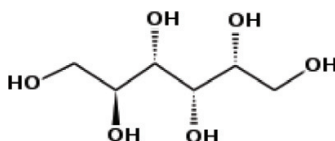
Figure 4. TG-DTG curve of xylitol under high-purity nitrogen.

4. Thermodynamic properties of nature sorbitol: C₆H₁₄O₆ [(CH₂OH)(CHOH)₄(CH₂OH), CAS No. 50-70-4]

4.1. Sample

The sorbitol sample was purchased from YuanJu Bio-Tech Co. Ltd. Shanghai, in PR China with batch number 040603 and labeled purity >99.0% mass fraction. The sample was recrystallized and then purified by sublimation. It was handled in a dry N₂ atmosphere to avoid possible contamination by moisture.

The chemical structure of sorbitol is as follows:



The mass of the sorbitol sample used for the heat capacity measurement is 3.71682 g, which is equivalent to 20.403 m mol based on its molar mass of 182.17165 g·mol⁻¹.

The mass of the sorbitol sample used in the DSC and TG experiment is 3.01 mg and 13.15 mg, respectively.

4.2. Results and discussion

4.2.1. Heat capacity

Experimental molar heat capacities of sorbitol measured by the adiabatic calorimeter over the temperature range from 80 to 390 K are listed in Ref. [18] and plotted in **Figure 5**. From **Figure 5**, a phase transition was observed in the range of 360–375 K with a peak temperature of 369.157 K. According to its melting point 366.5 K [7], this transition corresponds to a solid-liquid phase change.

The values of experimental heat capacities can be fitted to the following polynomial equations with least square method:

For the solid phase over the temperature range 80–355 K:

$$C_{p,m}/\text{J} \cdot \text{K}^{-1} \cdot \text{mol}^{-1} = 170.17 + 157.75x + 128.03x^2 - 146.44x^3 - 335.66x^4 + 177.71x^5 + 306.15x^6 \quad (9)$$

where x is the reduced temperature $x = [T - (T_{\max} + T_{\min})/2]/[(T_{\max} - T_{\min})/2]$, T is the experimental temperature, thus, in the solid state (80–355 K), $x = [(T/\text{K}) - 217.5]/137.5$, T_{\max} is the upper limit (355 K) and T_{\min} is the lower limit (80 K) of the above temperature region. The correlation coefficient of the fitting $R^2 = 0.9966$.

For the liquid phase over the temperature range 375–390 K:

$$C_{p,m}/\text{J} \cdot \text{K}^{-1} \cdot \text{mol}^{-1} = 518.13 + 3.2819 x \quad (10)$$

where x is the reduced temperature, $x = [(T/\text{K}) - 382.5]/7.5$, T is the experimental temperature, 382.5 is obtained from polynomial $(T_{\max} + T_{\min})/2$, 7.5 is obtained from polynomial $(T_{\max} - T_{\min})/2$. T_{\max} and T_{\min} are the upper (390 K) and lower (375 K) limit temperatures, respectively. The correlation coefficient of the fitting $R^2 = 0.9968$.

The heat capacity polynomials (9), (10) were used to calculate the smoothed heat capacities, and were numerically integrated to obtain the values of the standard thermodynamic functions above $T = 298.15$ K. The calculated results are listed in Ref. [18].

4.2.2. The temperature, enthalpy, and entropy of solid-liquid phase transition

The molar enthalpies and entropies of the solid-liquid phase transition $\Delta f_{\text{us}}H_m$ and $\Delta f_{\text{us}}S_m$ of sorbitol were derived according to the thermodynamic equations (see Section 4.2.2 in this chapter). The derived thermodynamic parameters were listed in Ref. [18].

4.2.3. Thermodynamic functions of sorbitol

The thermodynamic functions of the sorbitol relative to the reference temperature 298.15 K were calculated in the temperature range 80–390 K with an interval of 5 K, using the polynomial equations of heat capacity (9), (10) and thermodynamic relationships (see Section 2.2.2. in this chapter).

The calculated thermodynamic functions, $H_T - H_{298.15}$, $S_T - S_{298.15}$, are listed in Ref. [18].

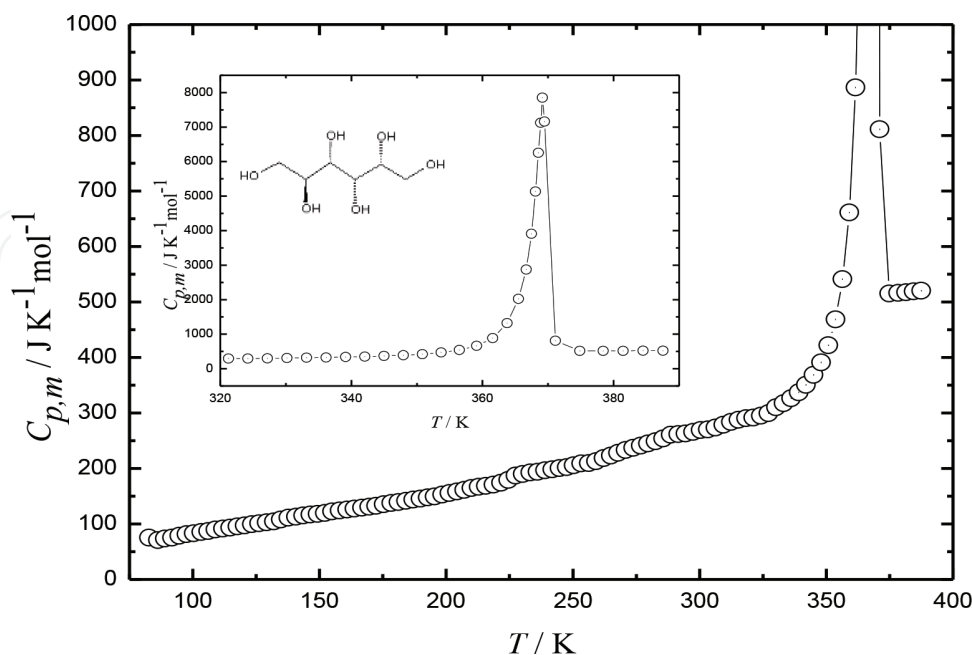


Figure 5. Experimental molar heat capacity of sorbitol as a function of temperature.

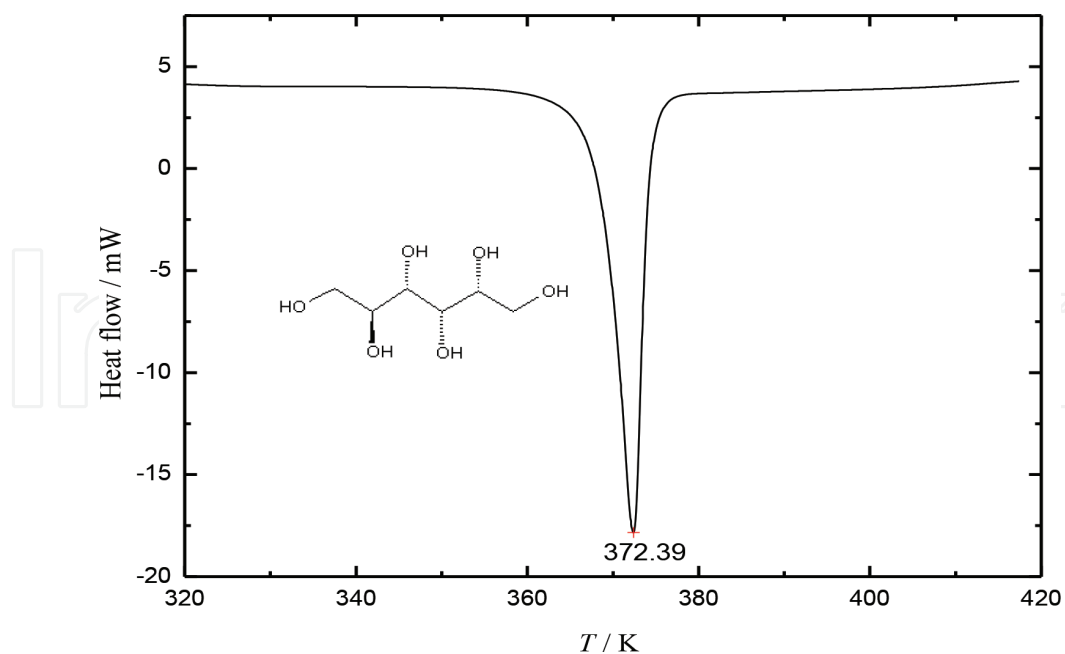


Figure 6. DSC curve of sorbitol under high-purity nitrogen.

4.2.4. The result of TG and DSC analysis

From the DSC curve in **Figure 6**, a sharply endothermic peak corresponding to melting process was observed, with the peak temperature of 372.39 K and the enthalpy of 30.66 ± 0.31 $\text{kJ}\cdot\text{mol}^{-1}$, which are consistent with the values (369.157 K, 30.35 ± 0.15 $\text{kJ}\cdot\text{mol}^{-1}$) observed from the adiabatic calorimetric measurements. The results were listed in Ref. [18], from which it can be seen that the thermodynamic parameters obtained from adiabatic calorimetry and DSC in the present research are in accordance with each other and slightly higher than those reported in literature [7].

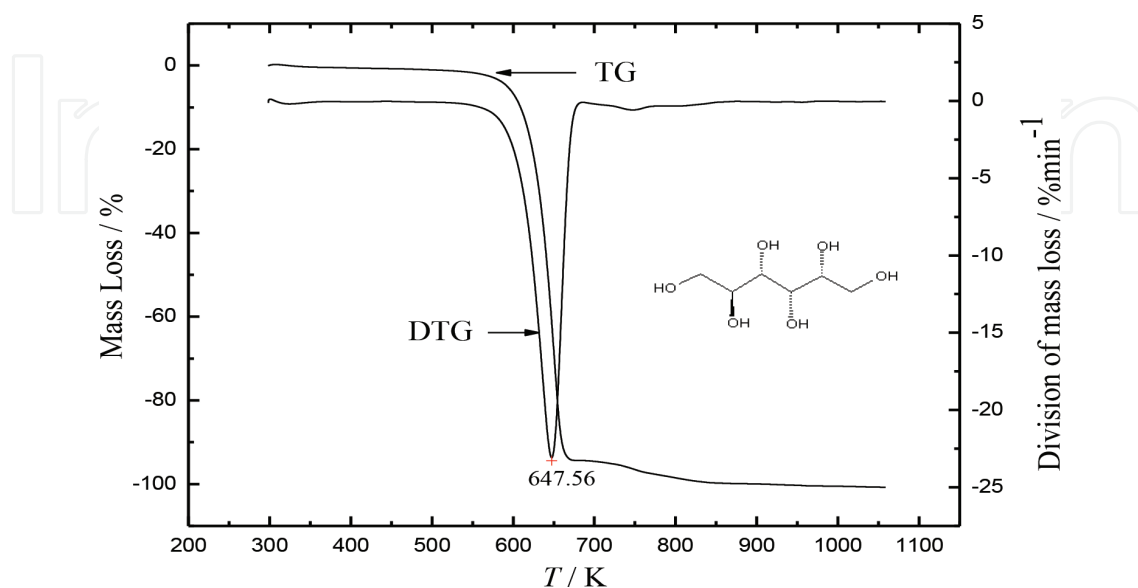


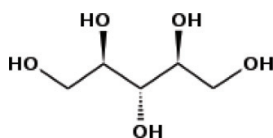
Figure 7. TG-DTG curve of sorbitol under high-purity nitrogen.

From the TG-DTG curve in **Figure 7**, it can be seen that the mass loss of the sample was completed in a single step. The sample keeps thermostable below 500 K. It begins to lose weight at 529.50 K, reaches the maximum rate of weight loss at 647.56 K, and completely loses its weight when the temperature reaches 764.50 K.

5. Thermodynamic properties of nature adonitol: $C_5H_{12}O_5$ [(CH₂OH)(CHOH)₃(CH₂OH), CAS No. 488-81-3]

5.1. Sample

The adonitol sample was purchased from ACROS ORGANICS Company with labeled purity of 99.0% mass fraction and was handled in a dry N₂ atmosphere to avoid possible contamination by moisture. GC analyses of the samples gave purities >99.0% in agreement with their specifications. The sample was used without additional purification. The chemical structure of adonitol is as follows:



The sample amount used for the heat capacity measurement is 2.27977 g, which is equivalent to 14.984 mmol based on its molar mass of 152.1457 g·mol⁻¹.

The mass of the sample used in the DSC experiment was 6–8 mg.

The mass of the sample used in the TG experiment was 11.72 mg.

5.2. Results and discussion

5.2.1. Heat capacity

Experimental molar heat capacities of adonitol measured by the adiabatic calorimeter over the temperature range from 78 to 400 K are listed in Ref. [21] and plotted in **Figure 8**. From **Figure 8**, a phase transition was observed at the peak temperature of 369.08 K. According to its melting point 374.7 K [7], this transition corresponds to a solid-liquid phase change. The values of experimental heat capacities can be fitted to the following polynomial equations with least square method: For the solid phase over the temperature range 78–360 K:

$$C_{p,m}^0 / J \cdot K^{-1} \cdot mol^{-1} = 170.000 + 98.817x + 23.846x^2 - 56.366x^3 - 92.259x^4 + 71.865x^5 + 82.678x^6 \quad (11)$$

where x is the reduced temperature $x = [T - (T_{\max} + T_{\min})/2] / [(T_{\max} - T_{\min})/2]$, T is the experimental temperature, thus, in the solid state (78–360 K), $x = [(T/K) - 219]/141$, T_{\max} is the

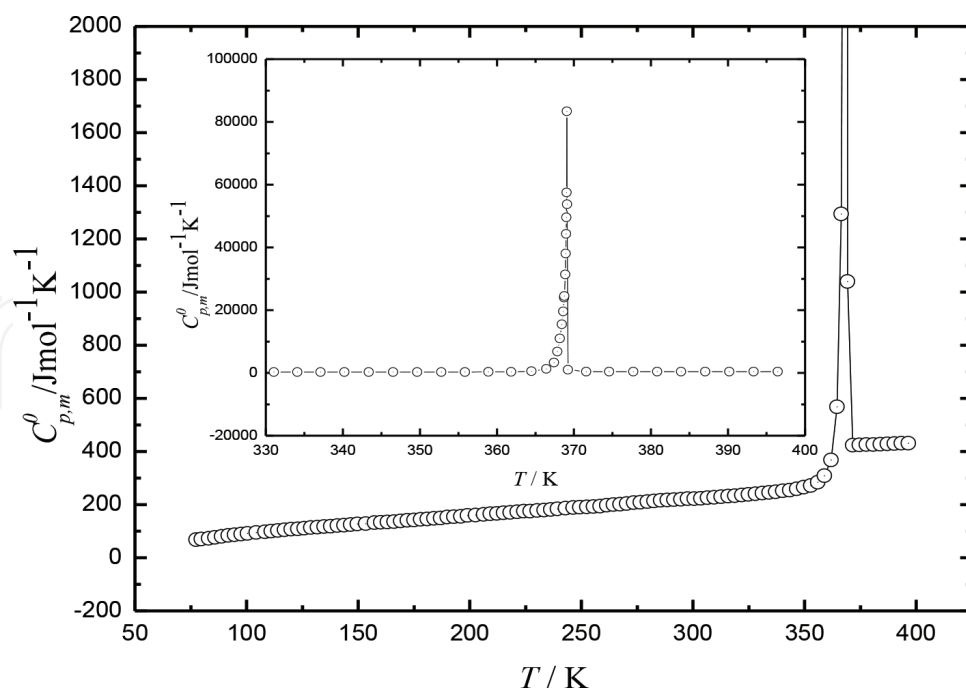


Figure 8. Experimental molar heat capacity of adonitol as a function of temperature.

upper limit (360 K), and T_{\min} is the lower limit (78 K) of the above temperature region. The correlation coefficient of the fitting $R^2 = 0.9986$.

For the liquid phase over the temperature range 375–400 K:

$$C_{p,m}^0 / \text{J} \cdot \text{K}^{-1} \cdot \text{mol}^{-1} = 428.460 + 3.821x \quad (12)$$

where x is the reduced temperature, $x = [(T/\text{K}) - 387.5]/12.5$, T is the experimental temperature, 387.5 is obtained from polynomial $(T_{\max} + T_{\min})/2$, 12.5 is obtained from polynomial $(T_{\max} - T_{\min})/2$. T_{\max} and T_{\min} are the upper (400 K) and lower (375 K) limit temperatures, respectively. The correlation coefficient of the fitting $R^2 = 0.9954$.

5.2.2. The temperature, enthalpy, and entropy of solid-liquid phase transition

The molar enthalpies and entropies of the solid-liquid phase transition $\Delta f_{\text{us}}H_m$ and $\Delta f_{\text{us}}S_m$ of adonitol were derived according to the thermodynamic equations (see Section 2.2.2 in this chapter). The derived thermodynamic parameters were listed in Ref. [21].

5.2.3. Thermodynamic functions of adonitol

The thermodynamic functions of the adonitol relative to the reference temperature 298.15 K were calculated in the temperature range 80–400 K with an interval of 5 K, using the polynomial equations of heat capacity (11), (12) and thermodynamic relationships (see Section 3.2.2. in this chapter).

The calculated thermodynamic functions, $H_T - H_{298.15}$ and $S_T - S_{298.15}$, are listed in Ref. [21].

5.2.4. The result of TG and DSC analysis

From the DSC curve in **Figure 9**, a sharply endothermic peak corresponding to melting process was observed, with the melting temperature of 373.61 ± 0.55 K and the enthalpy of 38.89 ± 1.17 kJ·mol⁻¹, which are slightly higher than the values 369.08 K, 36.42 ± 0.18 kJ·mol⁻¹ observed from the adiabatic calorimetric measurements and slightly lower than the values

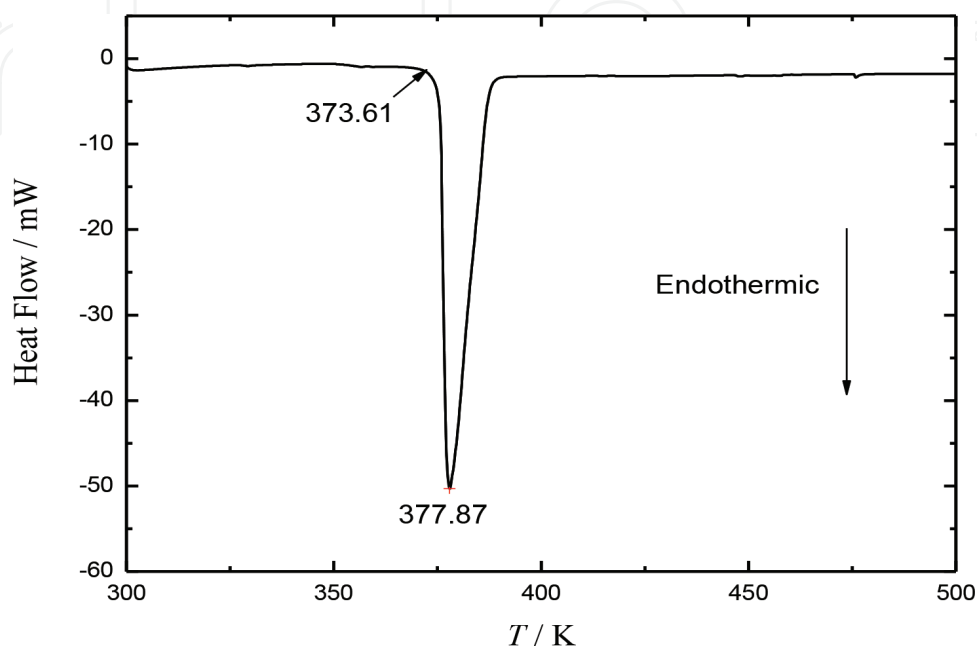


Figure 9. DSC curve of adonitol under high-purity nitrogen.

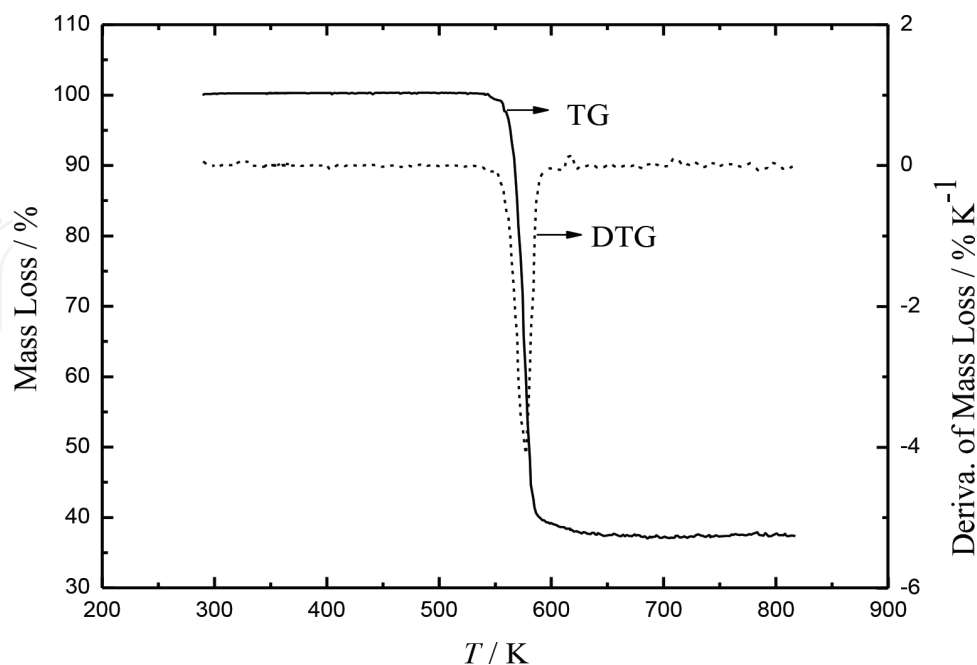


Figure 10. TG-DTG curve of adonitol under high-purity nitrogen.

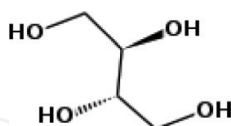
observed from DSC (374.7 K , $37.6\text{ kJ}\cdot\text{mol}^{-1}$) from G. Barone et al. in literature [7]. The results were listed in Ref. [21]. The data from DSC are obtained at a $10\text{ K}\cdot\text{min}^{-1}$ scanning rate, in which the sample could not reach thermal balance. However, the data of adiabatic calorimetry are obtained by means of the standard method of intermittently heating the sample and alternately measuring the temperature. The temperature difference between the sample and adiabatic shield was automatically kept to be about 10^{-3} K during the whole experiment. The temperature increment for a heating period was about 3 K , and temperature drift was maintained about 10^{-4} Kmin^{-1} during each equilibrium period. Therefore, this process is much more near to “adiabatic” and “balanced” than DSC method. Generally, the phase change temperature obtained from AC is lower than that from DSC.

From the TG-DTG curve in **Figure 10**, it can be seen that the mass loss of the sample was completed in a single step. The sample keeps thermostable below 550 K . It begins to lose weight at 551.55 K , reaches the maximum rate of weight loss at 577.38 K , and completely loses its weight when the temperature reaches 601.82 K .

6. Thermodynamic properties of nature erythritol: $\text{C}_4\text{H}_{10}\text{O}_4$ [(CH_2OH)(CHOH)₂(CH_2OH), CAS No. 149-32-6]

6.1. Sample

The erythritol sample was purchased from Shandong Baolingbao Biotechnology Co. Ltd. in PR China with batch number 060715 and labeled purity $>99.0\%$ mass fraction. The sample was recrystallized and then purified by sublimation. It was handled in a dry N_2 atmosphere to avoid possible contamination by moisture. Erythritol's molecular formula is $\text{C}_4\text{H}_{10}\text{O}_4$ with molar mass of $122.11975\text{ g}\cdot\text{mol}^{-1}$ and structural formula as follows:



The mass of the erythritol sample used for the heat capacity measurement is 4.76575 g , which is equivalent to 39.025 mmol based on its molar mass of $122.11975\text{ g}\cdot\text{mol}^{-1}$. The mass of the erythritol sample used in the DSC experiment was 9.70 mg . The mass of the erythritol sample used in the TG measurements was 18.35 mg .

6.2. Results and discussion

6.2.1. Heat capacity

Experimental molar heat capacities of erythritol measured by the adiabatic calorimeter over the temperature range from 80 to 410 K are listed in Ref. [20] and plotted in **Figure 11**. From

Figure 11, a phase transition was observed in the temperature range of 385–395 K with a peak temperature of 390.254 K.

The values of experimental heat capacities can be fitted to the following polynomial equations with least square method:

For the solid phase over the temperature range 80–385 K:

$$C_{p,m}/\text{J} \cdot \text{K}^{-1} \cdot \text{mol}^{-1} = 118.22 + 72.424X + 4.6835X^2 - 4.7788X^3 - 8.1937X^4 + 11.476X^5 + 4.48X^6 \quad (13)$$

where X is the reduced temperature $X = [T - (T_{\max} + T_{\min})/2]/[(T_{\max} - T_{\min})/2]$, T is the experimental temperature, thus, in the solid state (80–385 K), $X = [(T/\text{K}) - 232.5]/152.5$, T_{\max} is the upper limit (385 K) and T_{\min} is the lower limit (80 K) in the above temperature region. The correlation coefficient of the fitting $R^2 = 0.9998$.

For the liquid phase over the temperature range 395–410 K:

$$C_{p,m}/\text{J} \cdot \text{K}^{-1} \cdot \text{mol}^{-1} = 322.1 + 0.7507X \quad (14)$$

where X is the reduced temperature, $X = [(T/\text{K}) - 402.5]/7.5$, T is the experimental temperature, 402.5 is obtained from polynomial $(T_{\max} + T_{\min})/2$, 7.5 is obtained from polynomial $(T_{\max} - T_{\min})/2$. T_{\max} and T_{\min} are the upper (410 K) and lower (395 K) limit temperatures, respectively. The correlation coefficient of the fitting $R^2 = 0.9985$.

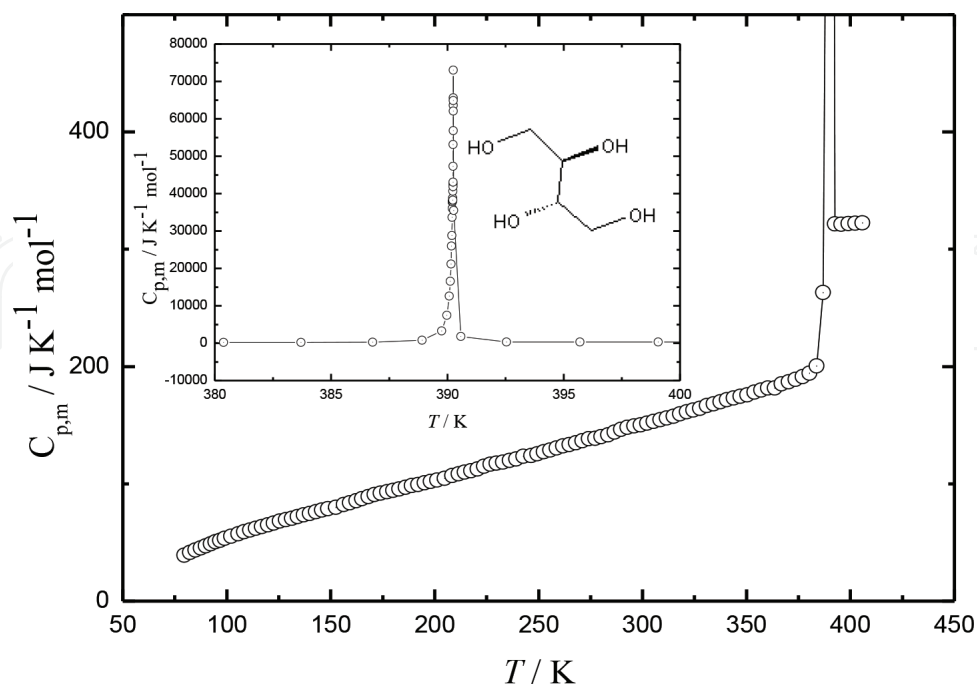


Figure 11. Experimental molar heat capacity of erythritol as a function of temperature.

6.2.2. The temperature, enthalpy, and entropy of solid-liquid phase transition

The molar enthalpies and entropies of the solid-liquid phase transition $\Delta f_{\text{us}}H_{\text{m}}$ and $\Delta f_{\text{us}}S_{\text{m}}$ of erythritol were derived according to the thermodynamic equations (see Section 3.2.2 in this chapter). The derived thermodynamic parameters were listed in Ref. [20].

6.2.3. Thermodynamic functions of erythritol

The thermodynamic functions of erythritol relative to the reference temperature 298.15 K were calculated in the temperature range 80–411 K with an interval of 5 K, using the polynomial equations of heat capacity (13), (14) and thermodynamic relationships (see Section 3.2.3. in this chapter).

The calculated thermodynamic functions, $H_{\text{T}} - H_{298.15}$ and $S_{\text{T}} - S_{298.15}$, are listed in Ref. [20].

6.2.4. The result of TG and DSC analysis

From the DSC curve in **Figure 12**, a sharply endothermic peak corresponding to melting process was observed, with the peak temperature of 397.33 K and the enthalpy of $34.89 \pm 0.35 \text{ kJ}\cdot\text{mol}^{-1}$, which are slightly lower than the values (390.254 K, $39.92 \pm 0.20 \text{ kJ}\cdot\text{mol}^{-1}$) observed from the adiabatic calorimetric measurements. The results were listed in Ref. [20], from which it can be seen that the thermodynamic parameters obtained from adiabatic calorimetry and DSC in the present research are in accordance with each other and slightly lower than those reported in literature [7].

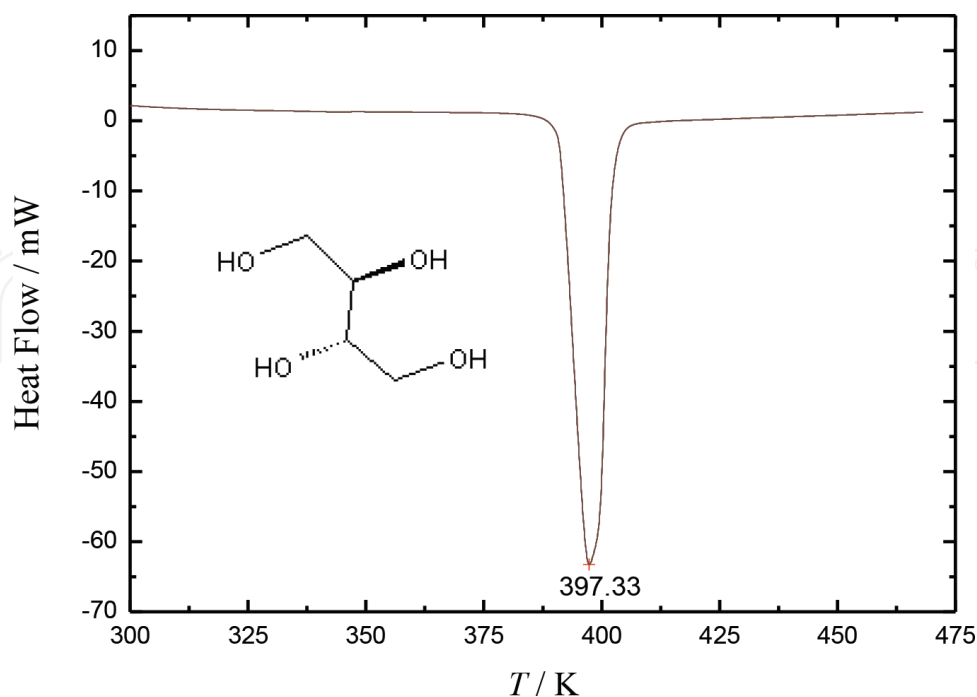


Figure 12. DSC curve of erythritol under high-purity nitrogen.

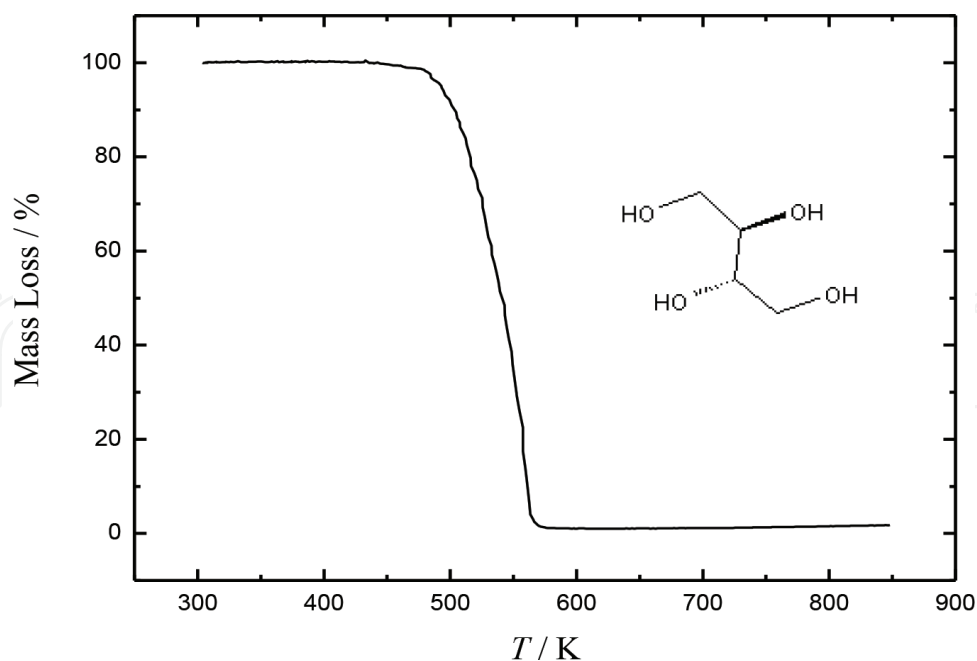


Figure 13. TG curve of erythritol under high-purity nitrogen.

From the TG-DTG curve in **Figure 13**, it can be seen that the mass loss of the sample was completed in a single step. The sample keeps thermostable below 450 K. It begins to lose weight at 476.75 K, reaches the maximum rate of weight loss at 557.44 K, and completely loses its weight when the temperature reaches 582.35 K.

7. Conclusion

In this chapter, the heat capacities of four kind of natural polyols, including xylitol, sorbitol, adonitol, and erythritol were measured in the temperature range from 80 to 400 K using a fully automated and high-precision adiabatic calorimeter constructed in our thermochemistry laboratory. The thermal stabilities of these polyols were also determined by thermal analysis techniques, differential scanning calorimeter (DSC), and thermogravimetric analyzer (TG). The heat capacity and thermodynamic property data presented in this chapter would provide a significant thermodynamic basis for understanding the thermal characteristics in both theory and practical designing of thermal energy storage units by using these polyols as PCMs. According to the above research results, the following conclusions can be drawn:

1. As the temperature of the polyols gradually increases, the solid-liquid phase change takes place, and the enthalpies of phase change are relatively large, hence, the polyols can be used as solid-liquid PCMs for thermal energy storage.
2. The phase change and thermostable temperature zone of the natural polyols covers 300 ~ 400 K, which is suitable for temperature control of human life and industrial production.

3. In the solid-liquid phase transition process, the thermodynamic properties of the natural polyols are stable, so their service life is long and convenient for practical application.
4. The natural polyols do not form plastic crystals, they are not volatile, are nontoxic, noncorrosive, so they can be used as a green and environment-friendly PCMs for thermal energy storage.
5. The key thermodynamic property data reported in this chapter for practical application of the four natural polyols as PCMs are finally summarized in **Table 1**.

Thermodynamic properties	Phase change temperature (K)	Enthalpy of phase change ($\text{kJ}\cdot\text{mol}^{-1}$)	Thermal stable temperature (<K)
Xylitol	369.04	33.26	450
Sorbitol	369.16	30.35	500
Adonitol	369.08	36.42	550
Erythritol	390.25	39.92	450

Table 1. Comparison of heat storage capacity of four natural polyols as solid-liquid phase change materials.

Acknowledgements

This work was financially supported by the National Natural Science Foundation of China under the grant NSFC No.21473198. Q. Shi would like to thank Hundred-Talent Program founded by Chinese Academy of Sciences.

Author details

Zhicheng Tan*, Quan Shi and Xin Liu

*Address all correspondence to: tzc@dicp.ac.cn

Thermochemistry Laboratory, Dalian Institute of Chemical Physics, Chinese Academy of Science, Dalian, China

References

- [1] Lan X-Z. A study on gelatinization and microencapsulation of low-temperature phase change materials for energy storage. Dalian Institute of Chemical Physics, Chinese Academy of Sciences, Dalian, China, 2003

- [2] Tong B. Preparation of polyols as phase change materials and studies on their thermodynamic properties. Dalian Institute of Chemical Physics, Chinese Academy of Sciences, Dalian, China, 2008
- [3] Tan ZC, Zhou LX, Chen SX, Li XY, Sun Y, Yin AX. A precision adiabatic calorimeter for measurement of heat capacities of aqueous solution of ethylene glycol. Chinese Science Bulletin. 1979;**24**:835-839
- [4] Benson DK, Burrows RW, Webb JD. Solid state phase transitions in pentaerythritol and related polyhydric alcohols. Solar Energy Materials. 1986;**13**:133-152
- [5] Zhang ZY, Yang ML. Heat capacities and phase transitions of 1,1,1-trihydroxymethylpropane and pentaerythritol over the superambient temperature range. Thermochimica Acta. 1989;**156**: 157-161
- [6] Zhang ZY, Yang ML. Heat capacity and phase transition of 2-amino-2-methyl-1,3-propanediol from 280K to the melting point. Thermochimica Acta. 1990;**169**:263-226
- [7] Barone G, Gatta GD. Enthalpies and entropies of sublimation, vaporization and fusion of nine polyhydric alcohols. Journal of Chemical Society Faraday Transaction. 1990;**86**(1):75-79
- [8] Granzow B. Hydrogen bonding and phase transitions of a group of alcohols derived from 2, 2-dimethylpropane. Journal of Molecular Structure. 1996;**381**:127-131
- [9] Takeda K, Yamamur O, Tsukushi I, Matsuo T, Suga H. Calorimetric study of ethylene glycol and 1,3-propanediol: Configurational entropy in supercooled polyalcohols. Journal of Molecular Structure. 1999;**479**:227-235
- [10] Li L, Tan ZC, Meng SH, Song YJ. A thermochemical study of 1,10-decanediol. Thermochimica Acta. 1999;**342**:53-57
- [11] Wang X, Lu ER, Lin WX, Liu T, Shi ZS, Tang RS, et al. Heat storage performance of the binary systems neopentyl glycol/pentaerythritol and neopentyl glycol/trihydroxy methyl-aminomethane as solid-solid phase change materials. Energy Conversion & Management. 2000;**41**:129-134
- [12] Wang XW, Lu ER, Lin WX, Wang CZ. Micromechanism of heat storage in a binary system of two kinds of polyalcohols as a solid-solid phase change material. Energy Conversion & Management. 2000;**41**:135-144
- [13] Feng HY, Xd L, He SM, Wu KZ, Zhang J. Studies on solid-solid phase transitions of polyols by infrared spectroscopy. Thermochimica Acta. 2000;**348**:175-179
- [14] Talja RA, Roos YH. Phase and state transition effects on dielectric, mechanical, and thermal properties of polyols. Thermochimica Acta. 2001;**380**:109-121
- [15] Romero CM, Páez M. Thermodynamic properties of aqueous alcohol and polyol solutions. Journal of Thermal Analysis and Calorimetry. 2002;**70**:263-267

- [16] Tong B, Tan ZC, Lv XC, Sun LX, Xu F, Shi Q, et al. Low-temperature heat capacities and thermodynamic properties of 2, 2-dimethyl-1, 3-Propanediol. *Journal of Thermal Analysis and Calorimetry*. 2007;**90**:217-222
- [17] Tong B, Tan ZC, Shi Q, Li YS, Wang SX. Thermodynamic investigation of several natural polyols (I). Heat capacities and thermodynamic properties of xylitol. *Thermochimica Acta*. 2007;**457**:20-26
- [18] Tong B, Tan ZC, Shi Q, Li YS, Wang SX. Thermodynamic investigation of several natural polyols (II). Heat capacities and thermodynamic properties of sorbitol. *Journal of Thermal Analysis and Calorimetry*. 2008;**91**:463-469
- [19] Tong B, Tan ZC, Wang SX. Low temperature heat capacities and thermodynamic properties of 2-methyl-2-Butanol. *Chinese Journal of Chemistry*. 2008;**26**:1561-1566
- [20] Tong B, Tan ZC, Zhang JN, Wang SX. Thermodynamic investigation of several natural polyols (III). Heat capacities and thermodynamic properties of Erythritol. *Journal of Thermal Analysis and Calorimetry*. 2009;**95**(2):469-475
- [21] Tong B, Yu Y, Tan ZC, Meng CG, Cuia LJ, Liu RB. Thermodynamic investigation of several natural polyols (IV):Heat capacities and thermodynamic properties of adonitol. *Thermochimica Acta*. 2010;**499**:117-122
- [22] Tong B, Tan ZC, Liu RB, Meng CG, Nan ZJ. Thermodynamic investigation of polyhydroxy solid-solid phase change materials (I): Heat capacities and standard molar enthalpy of formation of 2-Amino-2-methyl-1,3-propanediol ($C_5H_{11}NO_2$). *Energy Conversion and Management*. 2010;**51**:1905-1910
- [23] Tong B, Liu RB, Meng CG, Yu FY, Ji SH, Tan ZC. Heat capacities and nonisothermal thermal decomposition reaction kinetics of D-mannitol. *Journal of Chemical and Engineering Data*. 2010;**55**:119-124
- [24] Jia R, Sun KY, Li RC, Zhang YY, Wang WX, Yin H, Fang DW, Shi Q, Tan ZC. Heat capacities of some sugar alcohols as phase change materials for thermal energy storage applications. *Journal of Chemical Thermodynamics*. 2017;**115**:233-248
- [25] Sun KY, Kou Y, Li YS, Zheng H, Liu X, Tan ZC, Shi Q. Using silicagel industrial wastes to synthesize polyethylene glycol/silica-hydroxyl form-stable phase change materials for thermal energy storage applications. *Solar Energy Materials and Solar Cells*. 2018;**178**:139-145
- [26] Tan ZC, Liu BP, Yan JB, Sun LX. A fully automated high precision adiabatic calorimeter workable between 80 and 400 K. *Computers and Applied Chemistry*. 2003;**20**:264-268
- [27] Tan ZC, Shi Q, Liu BP, Zhang HT. A fully automated adiabatic calorimeter for heat capacity measurement between 80 and 400 K. *Journal of Thermal Analysis and Calorimetry*. 2008;**92**(2):367-374
- [28] Donald GA. Thermodynamic properties of synthetic sapphire standard reference material 720 and the effect of temperature-scale difference on thermodynamic properties. *Journal of Physical and Chemical Reference Data*. 1993;**22**:1441-1452